www.czasopisma.pan.pl PAN POLSKA AKADEMIA NAUK www.journals.pan.pl

A R C H I V E S O F M E T A L L U R G Y A N D M A T E R I A L S

Volume 57 2012 Issue 1

DOI: 10.2478/v10172-012-0030-7

Z. MALINOWSKI*, T. TELEJKO*, B. HADAŁA*

INFLUENCE OF HEAT TRANSFER BOUNDARY CONDITIONS ON THE TEMPERATURE FIELD OF THE CONTINUOUS CASTING INGOT

ANALIZA WPŁYWU WARUNKÓW BRZEGOWYCH NA POLE TEMPERATURY WLEWKA CIĄGŁEGO

Steel solidification in the continuous casting process starts in the mould, follows in the secondary cooling zones and finishes under air cooling conditions. Casting technology requires very effective heat transfer from the strand surface to the water cooling system. Design and control of the casting process is possible if the ingot temperature is known with a suitable accuracy. Measurements of the ingot temperature are complicated and expensive and due to these reasons are not common in practice. Numerical simulation have to be used to provide data which can be used to design and control of the ingot solidification. In the case of the temperature field modeling heat transfer boundary conditions have to be specified. In the literature wide range of formulas can be found and this may lead to essential errors in the heat transfer coefficient determination. In the paper the selected formulas have been employed in the finite element model to compute the ingot temperature field in the mould and secondary cooling zones. It has been shown that inaccurate determination of the heat flux transferred from the ingot surface to the mould leads to essential errors in the determination of the ingot temperature and solidification. Therefore empirical formulas or complex heat transfer models at ingot – mould interface ought to be employed in finite element models.

Keywords: heat transfer, boundary conditions, continuous casting

Krzepnięcie stali w procesie ciągłego odlewania zachodzi w krystalizatorze i strefie chłodzenia wtórnego. Technologia narzuca konieczność bardzo intensywnego odprowadzania ciepła od ciekłej stali, warstwy krzepnącej i zakrzepłej stali. Do prawidłowego prowadzenia odlewania konieczna jest znajomość wielu parametrów technologicznych, z których jednym z najważniejszych jest temperatura wlewka ciągłego. Bezpośrednie pomiary charakterystycznych dla COS wielkości w czasie krzepnięcia i stygnięcia wlewka są bardzo kosztowne oraz czasochłonne i z tych powodów nie znajdują szerszego zastosowania praktycznego. Najczęściej dane do analizy wpływu różnych parametrów wejściowych na proces krzepnięcia dostarczają symulacje numeryczne. Do prawidłowego ich wykonania potrzebne jest jednak określenie parametrów procesu. W przypadku temperatury bardzo ważną rolę odgrywają warunki brzegowe opisujące wymianę ciepła między powierzchnią wlewka ciągłego i otoczeniem. Ich niepoprawne przyjęcie może skutkować niedokładnym wyznaczeniem pola temperatury, a w konsekwencji błędami obliczeń pozostałych parametrów procesu. W literaturze często spotykane są różne formuły pozwalające na wyliczenie współczynnika przejmowania ciepła lub gęstości strumienia ciepła na powierzchni wlewka ciągłego. W pracy przedstawiono przykłady obliczeń pola temperatury dla wybranych zależności opisujących wymianę ciepła wlewka z otoczeniem w strefie krystalizatora i chłodzenia wtórnego. Przedstawiono wyniki symulacji oraz ich analizę. Obliczenia wykonano z zastosowaniem autorskiego modelu matematycznego i numerycznego wymiany ciepła oraz oprogramowania wykorzystującego metodę elementów skończonych.

1. Introduction

In the continuous casting process heat is transferred in three different modes: conduction, convection and radiation. In the liquid zone of a strand the main role plays convection and conduction. In the solid zone heat is transferred by conduction only. From the strand heat is transferred to the mould through the intermediate layer formed by solid and liquid casting powder and gases. In this layer all three mechanisms of heat transfer should be taken into consideration. Further, heat is conducted by a mould wall to the mould water cooling system. Below the mould strand is cooled in the secondary cooling section, where heat is extracted due to high pressure pulverized or air-atomized water sprays, radiation and contact with the back-up and guide rolls. In this zone heat transport is characterized by combined heat transfer coefficient. From the end of the secondary cooling

* AGH UNIVERSITY OF SCIENCE AND TECHNOLOGY, FACULTY OF METALS ENGINEERING AND INDUSTRIAL COMPUTER SCIENCE, 30-059 KRAKÓW, 30 MICKIEWICZA AV., POLAND

section to the cut-off section strand is cooled in air by convection and radiation mainly. It is also very important to include in the numerical model heat generation due to solidification and phase transformation in the solid state. Such complex problems of heat and mass transfer are very difficult to numerical modeling. The first numerical models have neglected heat convection [1]. This simplify the problem to heat conduction in opaque rigid body only. Heat transfer due to liquid motion has been taken into account replacing heat conduction by the effective heat conduction coefficient calculated based on a solid and liquid fraction of steel. The solutions have been limited to a mould zone and did not found practical implementation. Essential improvement have given three dimensional models where mass movement have been replaced by the resultant average velocity equal to casting speed [2,3]. This types of models give temperature field and solidified layer thickness close to transient solutions which take into consideration local velocities. Models based on average mass movement are not suitable to analyze problems caused by liquid steel motion in mould but are well suited to design mould cooling systems and secondary cooling section [4]. To solve heat transfer problem we need to specify initial condition, which defines the temperature distribution in the strand. Initial condition can be specified as body temperature equal to casting temperature. Boundary conditions required to solve heat transfer in the mould region are determined by the boundary layer which is formed between mould wall and solid or liquid steel. This boundary layer can be decomposed into zone of mould contact with liquid steel near the meniscus level and with solid layer at some distance below the meniscus. Further, the gap filed with gasses is formed between the mould and solid layer as distance from the meniscus increases. The highest local values of heat flux are observed near the meniscus. Measurements performed on industrial casters have given local values of heat flux from 1.5 MW/m^2 to 5 MW/m^2 [5,6] at the meniscus level. Heat transfer coefficient calculated based on Nusselt number for typical liquid steel and mould temperatures are in the range from 1 kW/(m^2 · K) to 4 kW/(m^2 · K). In numerical simulations heat transfer coefficients from 1 kW/(m^2 · K) [7] to 2.5 kW/(m^2 · K) [8] are employed very often.

2. Heat transfer model

Heat transfer in the system composed of cast strand, casting mould and environment has been modeled. The temperature field in the strand while cooling in the continuous casting mould, in the secondary cooling zones and in air has been determined from Fourier-Kirchhoff equation. It is possible to use transient or steady-state form of the heat transfer equation. Transient models are more general and give the possibility to simulate initial stage of casting processes while the mould is filled with liquid steel. However, the computation time in the case of transient three dimensional models is very long. Implementation of steady-state models gives the possibility to reduce computation time by at least hundred times. Further, the solution accuracy can be controlled by heat balance computed in the control volume. Due to this advantages in the developed model steady-state form of convection-diffusion heat transfer equation has been employed:

$$v_x\frac{\partial T}{\partial x}+v_y\frac{\partial T}{\partial y}+v_z\frac{\partial T}{\partial z}=\frac{\lambda}{\rho c}\left(\frac{\partial^2 T}{\partial x^2}+\frac{\partial^2 T}{\partial y^2}+\frac{\partial^2 T}{\partial z^2}\right)+\frac{q_v}{\rho c} \quad (1)$$

where:

T – temperature,
q_v – heat generation rate,
c – specific heat,
ρ – density,
λ – thermal conductivity,
v_x, v_y, v_z – velocity field components,
x, y, z – Cartesian coordinates,

In Eqn. (1) mass movement has been simplified and the resultant velocity of steel flow in the $y-z$ plane equal to casting speed v_o has been assumed. In such a case there is no steel movement along the axis of back-up rolls and the component of the velocity field v_x =0 has been assumed. In computational tests it has been noted that significant influence on solution stability has the heat of solidification. Heat generation rate q_v at element nodes can been calculated from:

$$q_v = Q_s\frac{dV_s}{d\tau} \quad (2)$$

where Q_s is heat of solidification, V_s represents volume of solid phase and τ is time. The solid phase volume has been computed from:

$$V_s = 1 - exp^{-K\frac{T_{li}-T}{T_{li}-T_{so}}} \quad (3)$$

where K is solidification kinetics constant, T is temperature, T_{li} , T_{so} are liquidus and solidus temperature, respectively. In Eqn. (2) derivative of V_s with respect to time can be estimated from the finite difference approximation:

$$q_v = Q_s\frac{\Delta V_s}{\Delta\tau} \quad (4)$$

With this approximation realistic results can be obtained in many technical problems in which internal heat source q_v is low if compared to the boundary heat flux. It is possible to use more complex method and calculate derivative of V_s taking into consideration solidified particle movement:

$$\frac{dV_s}{d\tau} = \frac{\partial T}{\partial l}\frac{\partial V_s}{\partial T}\frac{\partial l}{\partial \tau} \quad (5)$$

Performing partial differentiation with respect to particle path, temperature and time we have:

$$q_v = -Q_s \frac{\partial T}{\partial l} v_o \frac{K}{T_{li} - T_{so}} exp^{\frac{T_{li}-T}{T_{li}-T_{so}}} \tag{6}$$

In Eqn. (6) l represents distance measured along the particle path and v_o is particle velocity. The solution of Eqn. (1) gives the temperature field $T(x, y, z)$ which should satisfy the boundary conditions on the surface of the cast strand. The boundary condition have been specified in the form of heat flux transferred from the strand surface [9]:
– to the mould

$$q_{sk} = \alpha_{sk} (T_s - T_k) \tag{7}$$

– to water sprays

$$q_{sp} = \alpha_{sp} \left(T_s - T_p\right) \tag{8}$$

– to surroundings

$$q_c = \alpha_c (T_s - T_a) = (\alpha_{ra} + \alpha_{co}) (T_s - T_a) \tag{9}$$

where: T_s – strand surface temperature, T_p – water spray temperature, T_k – mould surface temperature from the side of strand, T_a – air temperature, α_{sk} – combined heat transfer coefficient on the strand – mould interface, α_{sp} – heat transfer coefficient for water spray cooling, α_c – combined heat transfer coefficient for air cooling including convection α_{co} and radiation α_{ra} components, respectively.

The solution of the strand cooling problem is possible if mould surface temperature is known. The mould takes heat from the cast strand surface and transfers it to the water cooling system at the outside surface of the mould. The mould temperature has been calculated from the transient heat conduction equation:

$$\frac{\partial T}{\partial \tau} = \frac{\lambda}{\rho c} \left(\frac{\partial^2 T}{\partial x^2} + \frac{\partial^2 T}{\partial y^2} + \frac{\partial^2 T}{\partial z^2} \right) \tag{10}$$

Boundary conditions on the mould surface have been specified in the following way:
– on the inner side which is taking heat from the strand – Eqn. (7):
– on the outer side S_w cooled by water:

$$q_w = \alpha_w (T_{kz} - T_w) \tag{11}$$

where: T_w – average water temperature in the mould cooling channel, T_{kz} – surface temperature of the outer side of the mould, α_w – heat transfer coefficient on the mould surface cooled by water.

3. Numerical simulations

The influence of cooling conditions on the strand temperature field have been analyzed for the square strand of 160mm×160mm in size. Chemical composition of steel has been assumed for the calculation as: 0.82%C, 2%Mn, 1.8%Si, 1.5%Co. Solidus temperature T_{so} was assumed as 1380°C, liquidus temperature T_{li} as 1480°C. The analysis has been performed for the arc of casting machine equal to 10 m. Casting speed was assumed as 30 mm/s. The length of the secondary cooling section was equal to 4.6 m. Computation have been performed for the water spray cooling section characterized in Table 1.

TABLE 1
Parameters of the water spray cooling section

Parameter / Zone number	Zone 1	Zone 2	Zone 3	Zone 4
Water spray flux rate $\dot{w}$, $dm^3/(m^2 \cdot s)$	5	3.5	3	1.5
Length of the water spray cooling zone, m	0.3	0.67	0.84	2.5

Influence of the heat transfer boundary conditions specified at strand – mould interface on the strand and casting mould temperature fields have been analyzed. Simulations have been performed for four variants of the combined heat transfer coefficient α_{sk} definition. In the simulation S1 constant heat transfer coefficient α_{sk} = 2000 W/(m^2 · K) at the strand mould interface has been employed. In the case of simulation S2 it has been assumed that heat is transferred from the strand to the mould by radiation only. In this case the heat transfer coefficient has been calculated from the equation:

$$\alpha_{sk} = \alpha_r = 5.67\, 10^{-8} \frac{\varepsilon_s \varepsilon_k}{\varepsilon_s + \varepsilon_k - \varepsilon_s \varepsilon_k} \frac{T_s^4 - T_k^4}{T_s - T_k} \tag{12}$$

Mould surface emissivity $\varepsilon_k = 0.6$ has been assumed. Strand surface emissivity has been calculated from the formula [10]:

$$\varepsilon_s = 1.1 + \frac{T_s - 273}{1000} \left(0.125 \frac{T_s - 273}{1000} - 0.38 \right) \tag{13}$$

In the case of simulation S3 combined heat transfer coefficient which takes into account conduction, convection and radiation has been calculated from the empirical formula:

$$\alpha_{sk} = \alpha_r + (\alpha_l - \alpha_r) exp^{\frac{T_s - T_{li}}{T_{so} - T_{za}}} \tag{14}$$

Below the meniscus level molten metal flows over the mould wall and convection is the main mechanism of heat transfer. It has been assumed that for the strand surface temperature greater than liquidus temperature T_{li} heat transfer is dominated by convection and $\alpha_{sk} = \alpha_l$ = 2000 W/(m^2 · K). Due to rapid cooling of the laminar

layer of the liquid steel solidification starts and a gap between steel and mould is formed. For fully developed gap heat transfer mechanism changes to radiation. Thus, two boundaries for the heat transfer coefficient can be prescribed. The upper bound is defined by the convection heat transfer coefficient α_l at the liquid steel – mould interface and the lower bound by the radiation heat transfer coefficient α_r in the gap. In the intermediate state the combined heat transfer coefficient described by Eqn. (14) depends on the steel liquidus and solidus temperatures and on the mould powder solidification temperature T_{za}. It has been assumed $T_{za} = 1150°C$ in simulation S3.

In several papers [11-14] heat transfer between strand and mould is associated with a slag formed by a casting powder. Slag is formed at the solidified steel layer. At the strand surface slag is in liquid state and due to rapid cooling is transformed into solid form near the mould wall. At some distance below the meniscus level gap filled with gases is formed which significantly increases the thermal resistance of the intermediate layer between the strand and mould wall. Scheme of the thermal resistance network for the heat transfer through the intermediate layer between the strand surface and the mould wall has been presented in Fig. 1. The thermal resistance of the intermediate layer is composed of the liquid and solid slag resistance and the resistance of gas layer. The slag layer is characterized by the thickness d_{za} and thermal conductivity λ_{za}. Heat transfer due to conduction through the slag layer is accomplished by radiation and the overall heat transfer coefficient in the case of simulation S4 has been calculated for the formula:

$$\alpha_{sk} = \frac{1}{R_{\sum}} \tag{15}$$

In Eqn. (15) $R_{\sum}$ represents the thermal resistance of the intermediate layer between the strand and mould wall. It is composed of thermal resistance of the gas gap R_{int} and the thermal resistance of the slag R_{eff}. The slag resistance R_{eff} can be decomposed into parts which are responsible for the heat transfer due to conduction in the liquid R_{liq}^{con} and solid R_{solid}^{con} layer and the radiation component R_{eff}^{rad}. The relations for this components can be expressed as:

$$R_{\sum} = R_{int} + R_{eff} \tag{16}$$

$$\frac{1}{R_{eff}} = \frac{1}{R_{eff}^{cond}} + \frac{1}{R_{eff}^{rad}} \tag{17}$$

$$R_{eff}^{cond} = R_{sol}^{cond} + R_{liq}^{cond} = \frac{d_{za}}{\lambda_{za}} \tag{18}$$

$$R_{eff}^{rad} = \frac{1}{\alpha_{rad}} \tag{19}$$

In Eqn. (19) the effective heat transfer coefficient due to radiation α_{rad} can be calculated from:

$$\alpha_{rad} = \frac{5.67\,10^{-8} n^2 \left(T_s^4 - T_{sm}^4\right)}{\left(0.75\beta d_{za} + \frac{1}{\varepsilon_{za}} + \frac{1}{\varepsilon_s} - 1\right)(T_s - T_{sm})} \tag{20}$$

In Eqn. (20) β is the average absorptivity for the total wavelength of thermal radiation, ε_{za} represents the emissivity of the solid slag and ε_s is the emissivity of the strand surface. Parameter n represents the reflectivity index of the thermal radiation in the slag layer. The temperature of the solid slag layer T_{sm} can be calculated from the surface energy balance:

$$\frac{T_{sm} - T_k}{R_{int}} = \frac{T_s - T_{sm}}{\frac{d_{za}}{\lambda_{za}}} \tag{21}$$

The thermal resistance of the gas gap can be determined in an empirical way [11-13] or can be calculated if the approximate thickness of the gas gap is known. The thermal resistance of the slag and gas gap varies in the range from 1 to 15 $(m^2 \cdot K)/W$. It depends on casting process parameters and the slag chemical composition [11,13]. The thermal resistance of the intermediate layer can be also calculated based on Cho [11] formula. Research conducted by Meng [14] can be used to calculate the mould powder thickness as a function of the distance from the meniscus:

$$d_{za} = 0.875z + 0.0006 \tag{22}$$

In Eqn. (22) z represents distance in meters measured from the meniscus level. In the case of simulation S4 it has been assumed: $R_{int} = 3 \cdot 10^{-4}$ $(m^2 \cdot K)/W$; λ_{za} =1.5 W/(m · K); n =1.5; β =250 1/m.

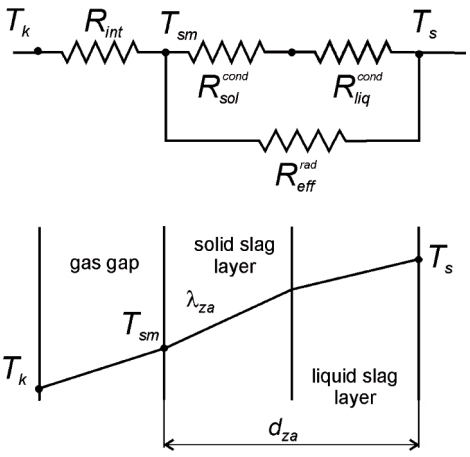

Fig. 1. The thermal resistance network for the heat transfer through the intermediate layer between the mould wall and strand surface

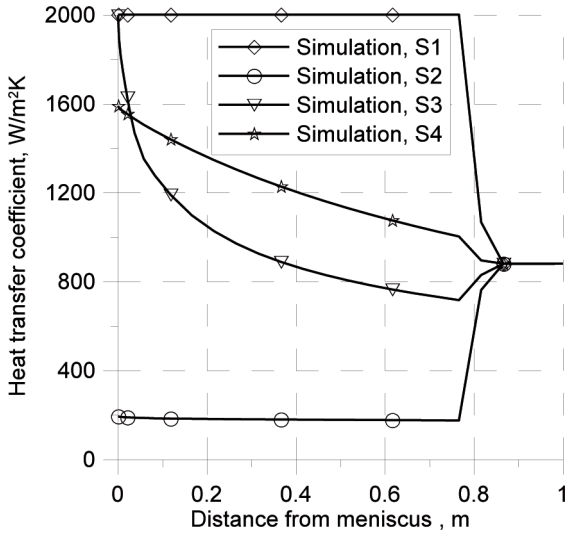

Fig. 2. Variation of the heat transfer coefficient at the strand mould interface for different heat transfer models

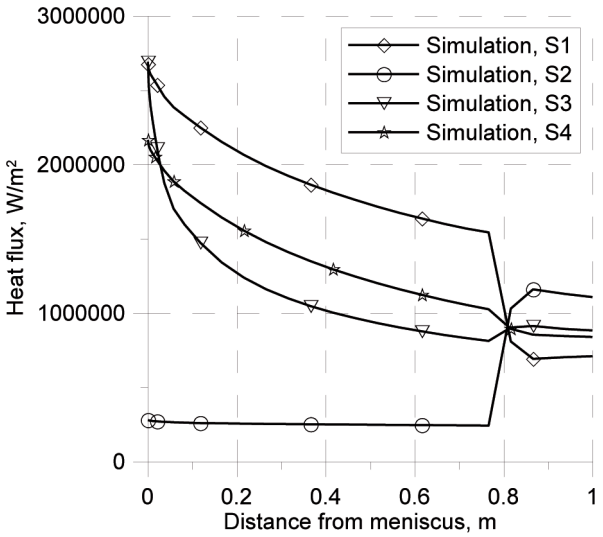

Fig. 3. Variation of the heat flux at the strand mould interface for different heat transfer models

The described four models of the heat transfer between the strand and the mould wall has been employed to compute the strand and mould temperature fields. The results of computations have been presented in figures from 2 to 9 as simulation: S1, S2, S3 and S4. In Fig. 2 variation of the effective heat transfer coefficient along the mould length has been shown. The upper boundary of the heat transfer from the strand to the mould is noted in the case of simulations S1 where thermal resistance of the gas layer has been neglected. In the opposite side the lower boundary for the heat transfer coefficient is noted in simulation S2 where the gas gap is assumed to exist from the meniscus level to the end of the mould. In this case the radiation heat transfer coefficient varies from 190 to 175 W/(m^2 · K). In the case of simulation S3 the empirical equation (14) has given the effective heat transfer coefficient in the range from 2000 at the meniscus level to 720 W/(m^2 · K) at the end of mould. The most complicated model described as simulation S4 has given the effective heat transfer coefficient in the range from 1600 at the meniscus level to 1000 W/(m^2 · K) at the end of mould. The local heat flux values at the strand – mould interface resulting from the models have been presented in Fig. 3. The model S1 has given unrealistic low heat flux. In the case of model S2 the heat flux is high but it can be achieved in some casters. The models S3 and S4 have given similar local values of the heat flux from the range of 2 MW/m^2 at the meniscus level to 1 MW/m^2 at the end of mould. The temperature variations along the centerline of the strand side surface have been presented in Fig. 4. The strand temperature of 1180°C and 1110°C has been obtained at the exit from the mould in the case of model S3 and S4, respectively. The results of computations given by models S3 and S4 are in the range of temperatures commonly noted in the industrial steel casters. Below the mould, the strand is cooled by water sprays and the cooling parameters have been given in Table 1. The water spray cooling has given the effective heat transfer coefficient in the range from 880 W/(m^2 · K) just below the mould to 420 W/(m^2 · K) at the end of the secondary cooling section, Fig. 6. The models S3 and S4 have given very similar heat flux values from 0.85 to 0.35 MW/m^2 in the secondary cooling zones. It should be noted that the same cooling parameters have been employed in simulations S1, S2, S3 and S4 in the water cooling section. It results in convergent heat fluxes at the end of the secondary cooling section, Fig. 7. Similar heat fluxes at the end of secondary cooling section result from the strand surface distribution presented in Fig. 8. The heat transfer models S1and S4 have given the strand surface temperature at the level of 1110°C and 1060°C at the end of the secondary cooling section, respectively. It is very important to note that the cooling model employed in the secondary cooling section, where the heat transfer coefficient is coupled with the strand surface temperature, reduced the difference in the strand surface temperature from 500°C at the end of mould to 50°C at the exit from the secondary cooling section for all computational variants. However, the implementation in numerical simulation of an appropriate heat transfer model between the strand and mould is critical in computation of the solid layer thickness along the mould. As it has been presented in Fig. 8 the models: S1, S2, S3 and S4 have given the solid layer thickness: 13mm, 2mm, 8mm and 9mm, respectively.

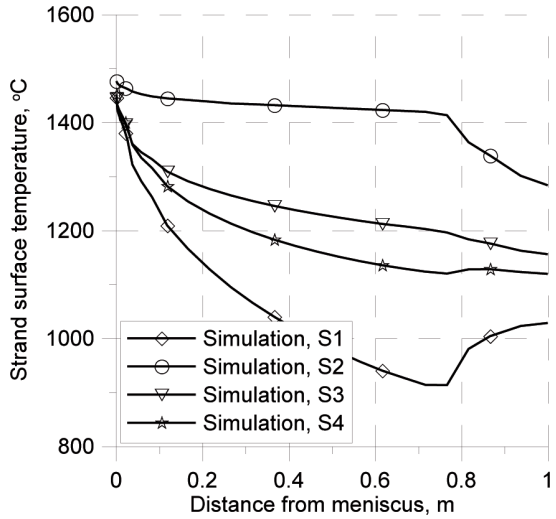

Fig. 4. Variation of the strand surface temperature along the mould length for different heat transfer models

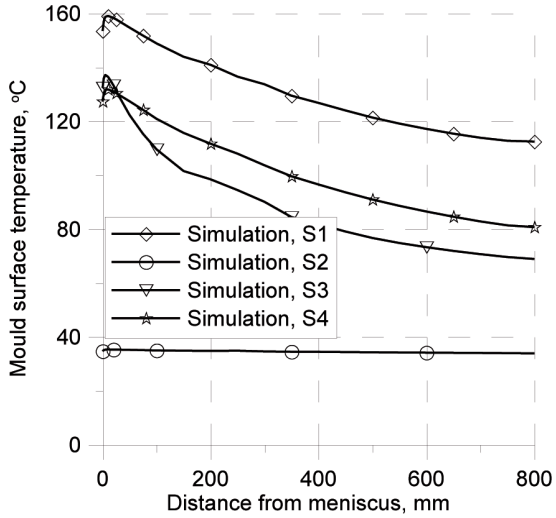

Fig. 5. Variation of the mould surface temperature along the mould length for different heat transfer models

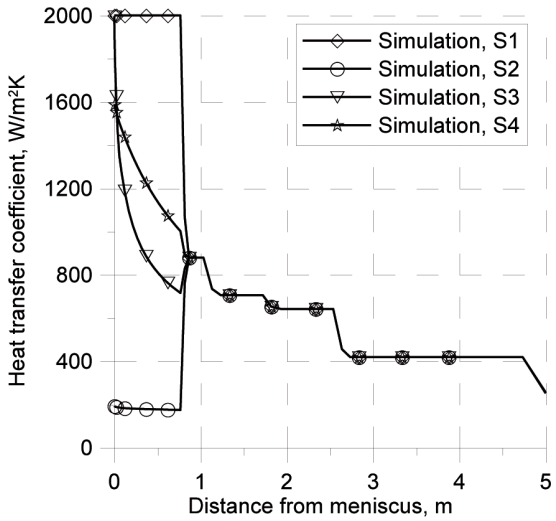

Fig. 6. Variation of the heat transfer coefficient along the strand length for different heat transfer models

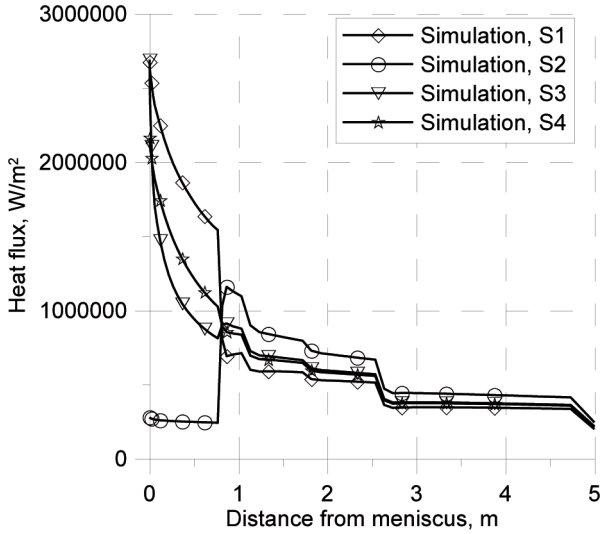

Fig. 7. Variation of the heat flux along the strand length for different heat transfer models

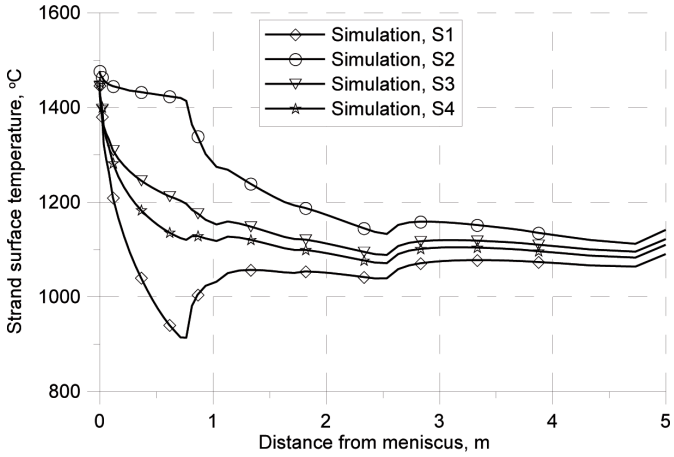

Fig. 8. Variation of the strand surface temperature along the strand length for different heat transfer models

4. Conclusions

The heat transfer between the strand and mould has been modeled with four different heat transfer boundary conditions. In the case of S1 model very good contact of the strand surface with the mould has been assumed. The opposite case has been described as S2 model where the gas gap along the mould length has been assumed. This two models have given the boundaries in the range of which the heat transfer in the steel casting process may be expected. In the secondary cooling section the differences in the strand surface temperature caused by different heat transfer models in the mould region have decreased significantly. This is possible due to higher heat flux taken out from the strand surface having higher temperature. In the models S3 and S4 combined heat

transfer due to conduction, convection and radiation has been taken into consideration. This models have given similar values of the effective heat transfer coefficient along the mould length. Parameters which are introduced in this models can be used to match heat transfer in industrial steel casters with good accuracy. Assumption of a constant heat transfer coefficient along the mould length may result in unrealistic description of the heat extraction from the strand surface. In consequence development of the solidified layer along the mould is not well determined. High differences in the strand temperature caused by inaccuracy in the heat transfer boundary conditions leads to essential errors in further simulations such as microstructure or fracture development.

Acknowledgements

Financial support of Structural Funds in the Operational Programme – Innovative Economy (IE OP) financed from the European Regional Development Fund – Project "New Concept for Selection the Cooling Parameters in Continuous Casting of Steel", POIG.01.03.01-12-009/09 is gratefully acknowledged.

REFERENCES

[1] J.K. Brimacombe, F. Weinberg, Ironmaking and Steelmaking **2**, 90 (1974).
[2] S.K. Choudhary, D. Mazumdar, A. Ghosh, ISIJ International **33**, 764 (1994).
[3] A.K. Tieu, I.S. Kim, Int. J. Mech. Sci. **39**, 185 (1997).
[4] T. Telejko, M. Rywotycki, Z. Malinowski, Archives of Metallurgy and Materials **4**, 837 (2009).
[5] K. Schwerdtfeger, Steel Research Int. **77**, 911 (2006).
[6] K. Schwerdtfeger, The Making, Shaping and Treating of Steel, Casting Volume, 11th ed., The AISE Steel Foundation 2003, 11.
[7] Y. Hebi, Y. Man, Journal of Materials Processing Technology **183**, 49 (2007).
[8] J.K. Park, B.G. Thomas, I.V. Samarasekera, Ironmaking and Steelmaking **29**, 359 (2002).
[9] B. Hadała, A. Cebo-Rudnicka, Z. Malinowski, A. Gołdasz, Archives of Metallurgy and Materials **56**, 367-377 (2011).
[10] C. Devadas, I.V. Samarasekera, Ironmaking and Steelmaking **13**, 311 (1986).
[11] J.W. Cho, T. Emi, H. Shibata, M. Suzuki, ISIJ International **38**, 834 (1998).
[12] A.C. Mikrovas, S.A. Argyropoulos, I.D. Sommerville, Ironmaking and Steelmaking **18**, 169 (1991).
[13] D.T. Stone, B.G. Thomas, Canadian Metallurgical Quarterly **38**, 363 (1999).
[14] Y. Meng, B.G. Thomas, Metallurgical and Materials Transactions B **34b**, 685 (2003).

Received: 10 September 2011.